JOURNAL OF GEOPHYSICAL RESEARCH, VOL. 115, D09111, doi:10.1029/2009JD012912, 2010

Evaluation of the observation operator Jacobian for leaf area index data assimilation with an extended Kalman filter

Christoph Rüdiger,[1,3] Clément Albergel,[2] Jean-François Mahfouf,[2] Jean-Christophe Calvet,[2] and Jeffrey P. Walker[1,3]

Received 28 July 2009; revised 20 December 2009; accepted 24 December 2009; published 14 May 2010.

[1] To quantify carbon and water fluxes between the vegetation and the atmosphere in a consistent manner, land surface models now include interactive vegetation components. These models treat the vegetation biomass as a prognostic model state, allowing the model to dynamically adapt the vegetation states to environmental conditions. However, it is expected that the prediction skill of such models can be greatly increased by assimilating biophysical observations such as leaf area index (LAI). The Jacobian of the observation operator, a central aspect of data assimilation methods such as the extended Kalman filter (EKF) and the variational assimilation methods, provides the required linear relationship between the observation and the model states. In this paper, the Jacobian required for assimilating LAI into the Interaction between the Soil, Biosphere and Atmosphere-A-gs land surface model using the EKF is studied. In particular, sensitivity experiments were undertaken on the size of the initial perturbation for estimating the Jacobian and on the length of the time window between initial state and available observation. It was found that small perturbations (0.1% of the state) typically lead to accurate estimates of the Jacobian. While other studies have shown that the assimilation of LAI with 10 day assimilation windows is possible, 1 day assimilation intervals can be chosen to comply with numerical weather prediction requirements. Moreover, the seasonal dependence of the Jacobian revealed contrasted groups of Jacobian values due to environmental factors. Further analyses showed the Jacobian values to vary as a function of the LAI itself, which has important implications for its assimilation in different seasons, as the size of the LAI increments will subsequently vary due to the variability of the Jacobian.

Citation: Rüdiger, C., C. Albergel, J.-F. Mahfouf, J.-C. Calvet, and J. P. Walker (2010), Evaluation of the observation operator Jacobian for leaf area index data assimilation with an extended Kalman filter, *J. Geophys. Res.*, *115*, D09111, doi:10.1029/2009JD012912.

1. Introduction

[2] For the purpose of carbon flux monitoring and weather forecasting, new-generation land surface models (LSM) have in the recent past been extended to include interactive vegetation components via a CO_2-responsive prognostic state in the form of photosynthetically active biomass [*Calvet et al.*, 1998; *Krinner et al.*, 2005; *Lafont et al.*, 2007]. The currently operational LSMs at Météo-France and the European Centre for Medium-Range Weather Forecasting (ECMWF) will be replaced in the foreseeable future by those new LSMs for use in numerical weather prediction. However, as for every dynamic model, the performance of the vegetation component in those models largely depends on the quality of input data and also on the model physics and parameterization [*Berg et al.*, 2003; *De Lannoy et al.*, 2007; *Walker et al.*, 2001]. Consequently, regular corrections are necessary through formalized data assimilation procedures, as both model predictions and observations suffer from uncertainties [*Crow et al.*, 2005; *Drusch et al.*, 2005; *Reichle et al.*, 2002].

[3] A number of studies have recently examined the potential of assimilating remotely sensed leaf area index (LAI) into these new LSMs in order to correct the vegetation biomass [*Dente et al.*, 2008; *Jarlan et al.*, 2008; *Sabater et al.*, 2008]. *Dente et al.* [2008] used a simple maximum likelihood function to minimize the differences between the observation and model state. Conversely, *Jarlan et al.* [2008] and *Sabater et al.* [2008] applied a simplified two-dimensional variational data assimilation scheme (2D-VAR) that was initially designed for the assimilation of screen level variables for the analysis of soil moisture states [*Balsamo et al.*, 2004], which is essentially a simplified extended Kalman filter, using the Jacobian to estimate the

[1]Department of Civil and Environmental Engineering, University of Melbourne, Parkville, Australia.
[2]Centre National de Recherches Météorologiques, Météo-France/CNRS, Toulouse, France.
[3]Now at Department of Civil Engineering, Monash University, Clayton, Victoria, Australia.

0148-0227/10/2009JD012912

sensitivity of model outputs to perturbations of the model's initial states, that is, at the beginning of the assimilation window. In the context of this data assimilation study, the Jacobian is the linearized model observation operator that projects the model states into the observation space. It is an essential cornerstone for the estimation of the Kalman gain matrix. Although these studies reported successful results, the Jacobian of the observation operator has not been examined in the detail necessary for numerical weather prediction (NWP) applications, in particular the requirement of short assimilation intervals (in the case of *Dente et al.* [2008], this is not applicable, as they did not apply a Kalman filter-type assimilation scheme). In atmospheric sciences, diagnostic studies of the Jacobian values have usually been performed before including new observation types in variational data assimilation systems [*Chevallier and Mahfouf*, 2001; *Fillion and Mahfouf*, 2003; *Garand et al.*, 2001] because it is essential to understand the sensitivity of the assimilation system before it is applied in an operational context. *Jarlan et al.* [2008] performed a sensitivity study of the behavior of the Jacobian values over a short time frame and showed that the system was linear only for relatively large (positive) perturbations of the LAI model state above 0.4 m^2/m^2 (this value defines the minimum value above which the Jacobian is independent of the perturbation size). The length of the assimilation window of the variational assimilation system (within which all available observations are assimilated) was chosen to 10 days. Longer assimilation windows of 50 days were also tested, but the tangent-linear approximation might be no longer valid. The choice of a relatively long assimilation window (i.e. 10 days), dictated by the current availability of satellite-derived LAI (operational LAI products are provided as 8 day composites), makes such surface assimilation incompatible with atmospheric data assimilation systems that have much shorter assimilation intervals (between 3 and 12 h). Focusing on the overall assimilation results of their 5 year study, *Jarlan et al.* [2008] did not study any seasonal effects in the underlying behavior of the assimilation system. Similarly, *Sabater et al.* [2008] studied a time period of 4 years (2001–2004) for a single site in southwestern France, concentrating their sensitivity study on the variability of the standard deviation of the Jacobian, which covered various ranges of perturbations. Through their study, they showed that those standard deviations do not vary significantly throughout a year, although they did not investigate the actual size of the Jacobian values themselves or their temporal evolution. Eventually, they also chose large perturbation sizes to estimate the Jacobian using finite-difference approximations (~0.5–1 m^2/m^2). As in the work of *Jarlan et al.* [2008], the assimilation window was also set to 10 days.

[4] *Mahfouf et al.* [2009] transformed the 2D-VAR used in the two previous studies to a comprehensive EKF for its operational use within the limited-area numerical weather prediction system Aladin of Météo-France [*Bubnová et al.*, 1995]. This new EKF version was then adapted for the purpose of this study to allow the joint assimilation of remotely sensed LAI and surface soil moisture observations for the analysis of the aboveground photosynthetically active vegetation biomass (B_a) and the root-zone soil moisture (w_2) within Interaction between the Soil, Biosphere and Atmosphere (ISBA)-A-gs [*Calvet et al.*, 1998], as previously proposed by *Sabater et al.* [2008]. Since the assimilation of surface soil moisture with EKF or ensemble Kalman filters has been discussed extensively [*Reichle et al.*, 2002; *Walker and Houser*, 2001; *Sabater et al.*, 2007], this aspect is not pursued here, and this paper focuses solely on the assimilation of LAI.

2. Description of Land Surface Model and Assimilation Scheme

2.1. Interaction Between the Soil, Biosphere and Atmosphere-A-gs Model

[5] The Interaction between the Soil, Biosphere and Atmosphere (ISBA) model [*Noilhan and Planton*, 1989; *Noilhan and Mahfouf*, 1996] is currently used operationally at Météo-France as the land surface component of their numerical weather forecasting models [*Giard and Bazile*, 2000]. A new version, ISBA-A-gs, has been developed to allow the assimilation of atmospheric CO_2 into the plant structure based on the stomatal conductance model of *Jacobs et al.* [1996], creating an interactive vegetation layer within the model [*Calvet et al.*, 1998]. This scheme was modified to improve the drought response of plants by *Calvet* [2000] and *Calvet et al.* [2004] (LST version). A biomass module was also introduced in ISBA-A-gs that can simulate the growth and mortality of the vegetation with different biomass reservoirs [*Calvet and Soussana*, 2001] (NIT version). The ratio α_B of the photosynthetically active aboveground biomass, B_a, over the LAI depends upon vegetation type, climate conditions, and nitrogen supply according to a plant nitrogen decline module [*Calvet and Soussana*, 2001], which was derived from the work of *Lemaire and Gastal* [1997]. This ratio, currently set to a constant value for the individual vegetation types within ISBA-A-gs, provides the link between the simulated observation (LAI) and the control variable of the system (B_a) that is closely related to the Jacobian of the EKF. During the growing phase of the vegetation (net CO_2 assimilation greater than mortality), the total aboveground biomass (sum of photosynthetically active and structural components) is derived from the active biomass through an allometric logarithm law based on a nitrogen decline model [*Calvet and Soussana*, 2001]. Therefore, under such conditions, any increase in active biomass is partly converted into structural (and therefore inactive) biomass in order to fulfill the allometric logarithm law. When the vegetation becomes senescent (mortality greater than net CO_2 assimilation), the nitrogen decline equations no longer apply: active and inactive biomass reservoirs evolve independently. The ISBA-A-gs version used in this study is the most recent version implemented into the land surface modeling platform SURFEX of Météo-France [*Le Moigne*, 2009].

2.2. Extended Kalman Filter

[6] A full description of the EKF applied in this study is given by *Mahfouf et al.* [2009], and the reader is referred to their paper for more details. Consequently, only key equations are presented in the following. The equation for the model state analysis is

$$\mathbf{x}_a^t = \mathbf{x}_b^t + \mathbf{B}\mathbf{H}^T\left(\mathbf{H}\mathbf{B}\mathbf{H}^T + \mathbf{R}\right)^{-1}\left[\mathbf{y}_o^t - h\left(\mathbf{x}_b^{t_0}\right)\right], \qquad (1)$$

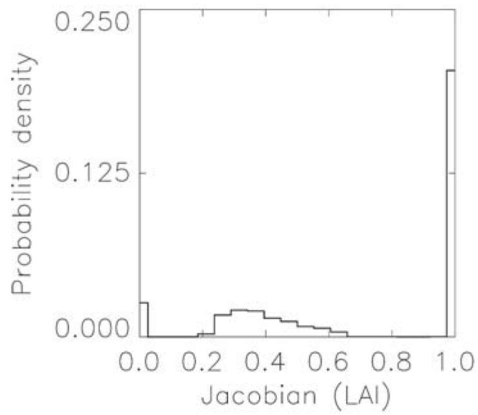

Figure 1. Histogram of leaf area index (LAI) Jacobian values obtained over a 7 year period (2001–2007) at the Surface Monitoring of Soil Reservoir Experiment (SMOSREX) experimental site (southwestern France), using the grassland parameterization. Those data were obtained from the Interaction between the Soil, Biosphere and Atmosphere (ISBA)-A-gs surface scheme and considering a 24 h assimilation interval.

where $\mathbf{x}$ is the model state and the superscripts a and b denote the analysis and background states, respectively; t is the time step indicator; $\mathbf{B}$ is the background error covariance matrix; $\mathbf{R}$ is the observation error covariance matrix; h is the observation operator; and $\mathbf{y}$ is the observation vector. In the particular case of this study, the model state $\mathbf{x}$ is the active biomass (B_a) and the observation $\mathbf{y}$ is the LAI.

[7] The Jacobian matrix $\mathbf{H}$ of the linearized observation operator is defined as

$$\mathbf{H} = \frac{\partial \mathbf{y}}{\partial \mathbf{x}}. \tag{2}$$

In this study the Jacobian matrix is estimated using a finite-difference approximation by perturbing the initial model state by a small amount $d\mathbf{x}$ and estimating the difference $d\mathbf{y}$ between a perturbed simulated observation $\mathbf{y} + d\mathbf{y}$ and a reference value $\mathbf{y}$. The optimal size of $d\mathbf{x}$ is examined hereafter. In practice, since a linear relationship exists between the LAI and B_a (LAI = B_a/α_B, with α_B being different for different biomes), the Jacobian is expressed as a function of LAI only:

$$h = \frac{d\mathrm{LAI}^t}{d\mathrm{LAI}^{t_0}}, \tag{3}$$

where t is the time at which the observation is available (usually the end of the assimilation interval) and t_0 is the initial time for which the control vector has to be corrected (usually the beginning of the assimilation interval). In this study the assimilation interval is defined as the time interval between t_0 and t in order to distinguish this from the assimilation window of a variational assimilation method.

[8] In its current form, the EKF assimilates observations over an interval of 24 h at 0600 LT, when available, by analyzing the initial state via the information provided by an observation at the end of the assimilation interval (i.e., the observation operator contains the forward model propagation and the conversion of the model state into an observation equivalent). The propagation of the background error covariance matrix by the tangent-linear forward model in the EKF is performed through the Jacobians ($\mathbf{M}$ and $\mathbf{M}^T$) of the forward model:

$$\mathbf{B}^t = \mathbf{M}\mathbf{B}^{t_0}\mathbf{M}^T + \mathbf{Q}, \tag{4}$$

where $\mathbf{Q}$ is the covariance matrix of model errors. This allows for observations to be available less frequently than the chosen assimilation interval length (thereby providing a similar solution as the simplified 2D-VAR [*Balsamo et al.*, 2004] over a long assimilation window but without making the assumption of a perfect model), as discussed in detail by *Draper et al.* [2009]. In the present study the propagation of the background error covariance matrix $\mathbf{B}$ is not essential for the understanding of the discussed results, as only the sensitivity of model states to initial perturbations are discussed, for which neither the information of the background nor the observation error covariance matrices is required.

3. Data

[9] While this is a synthetic experiment, inasmuch as there are no comparisons with real observations, all atmospheric forcing data were obtained from instrumentation installed at the Soil Monitoring of Soil Reservoir Experiment (SMOSREX) experimental site near Toulouse in southwestern France [*De Rosnay et al.*, 2006] for the 7 year period 2001–2007. The surface cover at this site consists of a wild growth of fallow. The climate in this area is described as temperate with relatively warm and dry summers, whereas the winter periods are cold and wet but generally snow-free at this site. Surface frost appears regularly throughout the winter and early springtime, while water stress is common in summer. The soil physical and plant physiological parameters of ISBA-A-gs have been assessed for this site in previous studies [e.g., *Sabater et al.*, 2008], and those parameters remain unchanged except for one. The cuticular conductance set to 0 mm/s by *Sabater et al.* [2008] is now set to 0.3 mm/s. This revised parameter value allows more plant water exchange with the model now being able to go below the wilting point in dry periods. In an additional study (see Section 4.5) the parameters were replaced by those of a deciduous broadleaf forest, to study the Jacobian for a different vegetation type.

4. Results

4.1. Jacobian Estimates

[10] The Jacobian of the observation operator h (as defined in equation (3)) required to estimate the Kalman gain of the analysis equation is computed using the finite-difference approximation as

$$h = \frac{f_{\mathrm{LAI}}^t(\mathrm{LAI}^{t_0} + d\mathrm{LAI}^{t_0}) - f_{\mathrm{LAI}}^t(\mathrm{LAI}^{t_0})}{d\mathrm{LAI}^{t_0}}, \tag{5}$$

where $f_{\mathrm{LAI}}^t(\cdot)$ is the modeled LAI at time t based on the model state $(\cdot)$ at time t_0; the small initial perturbation $d\mathrm{LAI}^{t_0}$ of the control variable is set to $\varepsilon\mathrm{LAI}^{t_0}$, with ε being a small numerical value.

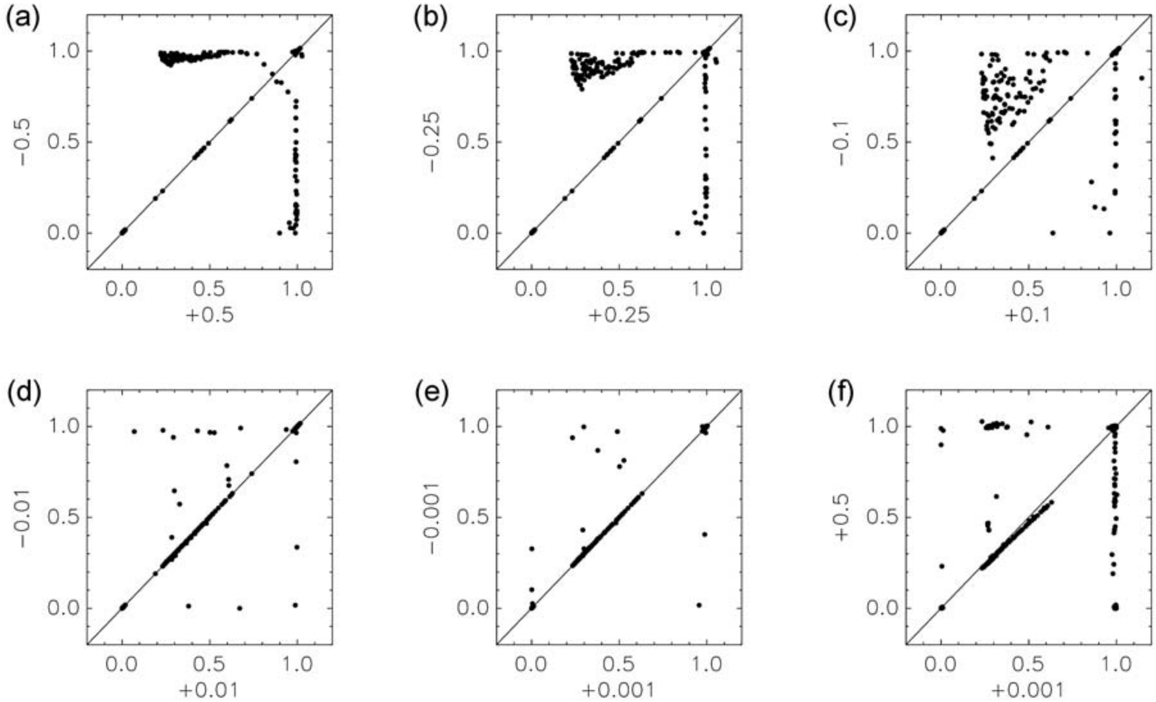

Figure 2. Scatterplots of daily LAI Jacobian values obtained in 2001 at the SMOSREX experimental site using a finite-difference approximation with perturbation sizes ε ranging from ±0.5 to ±0.001. (a–e) Plots of positive versus negative perturbations (identical absolute perturbations; linearity regime along the first diagonal). (f) Plot of Jacobian values obtained with the smallest positive perturbation against those obtained with the largest positive perturbation.

[11] Using a baseline value of $\varepsilon = 0.001$ (to be justified in the next section), the Jacobian values have been computed with a daily time step (i.e., $t - t_0 = 1$ day) over a 7 year period (2001–2007). The model is run in an open-loop configuration with no assimilation, for which the initial states are simply perturbed every 24 h. The Jacobian is therefore the difference in the prognostic states between perturbed and reference open-loop runs at the end of the assimilation interval, divided by the initial perturbation. The histogram of Jacobian values obtained over the 7 year period is displayed in Figure 1. Three different Jacobian "types" are identified corresponding to the three modes of the distribution: (1) identical to zero (Jacobian type O), representing 8% of the population, (2) values between 0.2 and 0.6 (Jacobian type A), representing 27% of the population, and (3) close to 1 (Jacobian type B), representing 65% of the population.

[12] The values of type B represent the situation in which the perturbation of the initial state results in the same offset at the end of the assimilation interval: in such situations a static analysis could prevail since the model dynamics is the identity (no influence of the time dimension). Conversely, for Jacobian values of type A, the final offset is only a fraction of the initial perturbation, which indicates that in such situations the model dynamics is strongly dissipative.

4.2. Sensitivity of the Jacobian to the Size of Initial Perturbations

[13] The sensitivity of the Jacobian to the size of the initial perturbations of the prognostic model state (B_a) is studied using 1 year of simulations performed for 2001. This period was chosen as it represents an average year in terms of the overall atmospheric conditions in southwestern France, with neither exceptionally dry or wet or extensive cold and hot periods. The perturbations were calculated using values of ε ranging from 0.001 to 0.5 (corresponding to LAI perturbations of about 0.003–2 m^2/m^2, depending on the season). Positive and negative perturbations were also considered in order to better examine the validity range of the Jacobian computation using the finite-difference approximations. It is important to mention that the EKF is based on the validity of the tangent-linear approximation and of the gaussianity of background and observation errors. Therefore, in situations in which these approximations break down, even if the Jacobian computation is accurate enough, the analysis will be suboptimal.

[14] Figure 2 presents scatterplots of Jacobian values obtained with positive and negative LAI perturbations for magnitudes of ε ranging from 0.001 to 0.5. For perturbations with ε smaller than 0.01 most of the points are aligned along the first diagonal, indicating similar Jacobian values when considering either positive or negative perturbations, which is the signature of an almost linear regime. For ε values larger than 0.01, the linearity regime breaks down since the vast majority of type A Jacobian values (between 0.2 and 0.6) are located outside the first diagonal. Therefore, perturbation values chosen by *Jarlan et al.* [2008] and *Sabater et al.* [2008] seem too large for this linear regime. Despite this finding, when plotting the Jacobian values obtained with a small positive value ($\varepsilon = 0.001$) against those

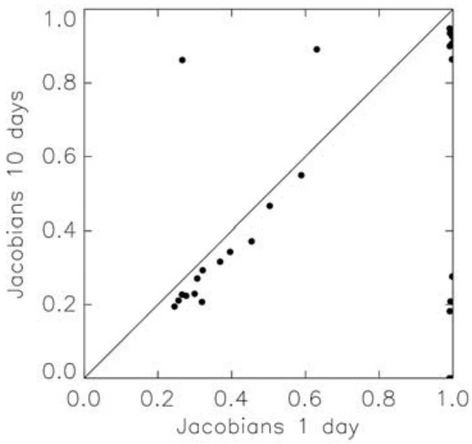

Figure 3. Scatterplot of LAI Jacobian values obtained in 2001 at the SMOSREX experimental site using a finite-difference approximation (ε = 0.001) with 10 day assimilation intervals versus 1 day assimilation intervals.

obtained with a large positive value (ε = 0.5) (Figure 2f) a significant number of points are aligned along the first diagonal, which corresponds to a similar number of Jacobian values of type A for both small and large perturbations. Thus, the linearity regime appears to be valid over a wider range of values for positive perturbations than for negative ones. In the remainder of this paper a small value for ε of 0.001 is therefore used, for which the Jacobian values estimated with positive and negative perturbations are very similar. Smaller perturbations lead to discrepancies between positive and negative values due to numerical round-off errors in the estimation of the Jacobian values (not shown).

4.3. Sensitivity of the Jacobian to the Length of the Assimilation Interval

[15] For comparison with previous studies, the Jacobian has also been computed for longer assimilation intervals of 10 days instead of the 1 day baseline initially used. A scatterplot of 10 day Jacobian values computed in 2001 (36 values) against corresponding 1 day Jacobian values (estimated over the last 24 h period of the 10 day assimilation interval) is shown in Figure 3. Except for two points, the 10 day values are systematically smaller than Jacobian values estimated over a 1 day period. Jacobian values of type A are slightly shifted below the first diagonal, and Jacobian values of type B over 10 days have values centered around 0.90 instead of 1.00. This behavior is expected as the 1 day values are generally just below or equal to one. Therefore, the convolution of Jacobian values over longer periods results in smaller or equal values than over 1 day (since they are combined as products). Larger Jacobian values over longer periods could only be obtained with 1 day values larger than 1 (amplifying modes). In that case the assimilation over longer intervals would be preferable since larger analysis increments could be obtained for a given value of the innovation vector. The use of an EKF over a short assimilation interval allows the introduction of a model error term **Q** in the evolution of the background covariance matrix **B** that can counteract the damping effect of the propagation by the tangent-linear model **M** (equal to h in our study) given by $\mathbf{MBM}^{\mathrm{T}}$. Such an increase of background errors was not envisaged in the simplified 2D-VAR systems of *Jarlan et al.* [2008] and *Sabater et al.* [2008], where a perfect model assumption was implicitly made (which can become questionable when integrating a numerical model over a long time window). Moreover the use of a short assimilation interval allows analyses to be delivered sooner for near-real-time NWP applications, since the simplified 2D-VAR needs observations to be made over the subsequent 10 days for estimating the LAI analysis of the present day.

4.4. Seasonal Variation of the Jacobian

[16] Assuming a slow evolution of the vegetation biomass over 1 day, it was unexpected to obtain Jacobian values of type A. Initially, only values of or near type B were expected, as intuitively the plant should not physically convert, create, or destroy relatively large quantities of active biomass in 1 day. However, an analysis of the model behavior showed that during the periods of type A Jacobian values, active biomass was converted into inactive (aboveground structural) biomass through the process of plant net carbon assimilation (nitrogen dilution concept), which explains the loss of active vegetation.

[17] The time series in Figure 4 shows the Jacobian over a 7 year period for the baseline perturbation ε of 0.001 together with the simulated LAI and root-zone soil moisture w_2. The soil water content at the wilting point w_{wilt} (0.17 m^3/m^3) is also displayed since it controls the effect of plant water stress in ISBA-A-gs. The annual cycle in the temporal evolution of the Jacobian values is clearly distinguished. As already defined, the Jacobian values behave as types O, A, and B, with the Jacobian values of type B existing only during periods of low vegetation growth or high mortality. These periods coincide with four different states of the model: (1) cold periods (winter season), (2) cloudy and rainy periods (corresponding to frequent changes in the Jacobian when $d\mathrm{LAI}/dt > 0$), (3) periods of vegetation senescence (when $d\mathrm{LAI}/dt < 0$), and (4) periods of water stress (when $w_2 < w_{\mathrm{wilt}}$). During all these periods, no or very little net assimilation of carbon into the plant system takes place. The third case of Jacobian values (type O) is identified during winter periods, when the Jacobian values are strictly zero. This situation occurs when the modeled LAI is set to an arbitrary small value of 0.3 m^2/m^2 due to the environmental conditions. In that case, the model prediction was independent of the initial state of the active biomass, leading to a zero Jacobian value. Finally, removing all Jacobian values of types O and B and plotting the remaining values against the modeled LAI yields a strong correlation between the two data sets (Figure 5).

[18] The presence of Jacobian values of type O suggest that an assimilation of LAI, when the model is required to reset the model to its minimum value of 0.3 m^2/m^2, is not sensible. The resulting type O Jacobian is not sufficiently informative, other than that the environmental conditions do not allow higher LAI values. However, this is not critical, as it is unlikely that the model will result in a large error during such periods (which can potentially also occur during extreme droughts in summer), as the vegetation is generally dormant.

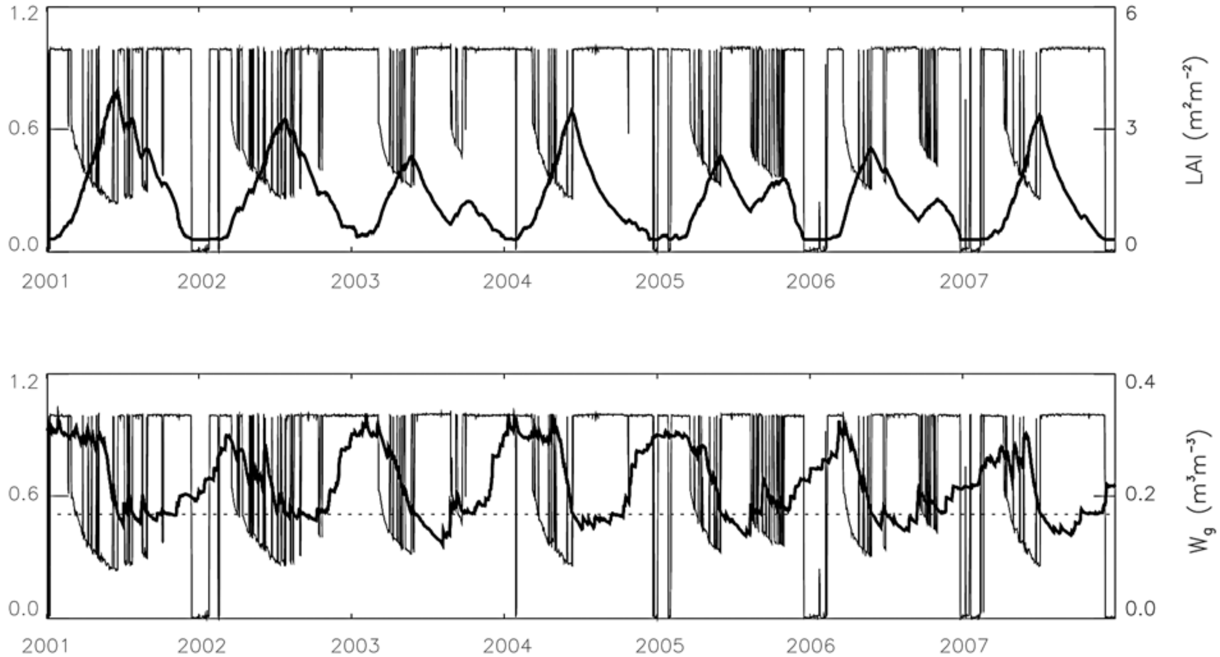

Figure 4. Time evolution of daily LAI Jacobian values (thin line) over a 7 year period (2001–2007) at the SMOSREX experimental site together with (top) simulated LAI (thick line) and (bottom) root-zone soil moisture (thick line) by the ISBA-A-gs surface scheme. The dashed line in Figure 4 (bottom) shows the value of the soil moisture at wilting point.

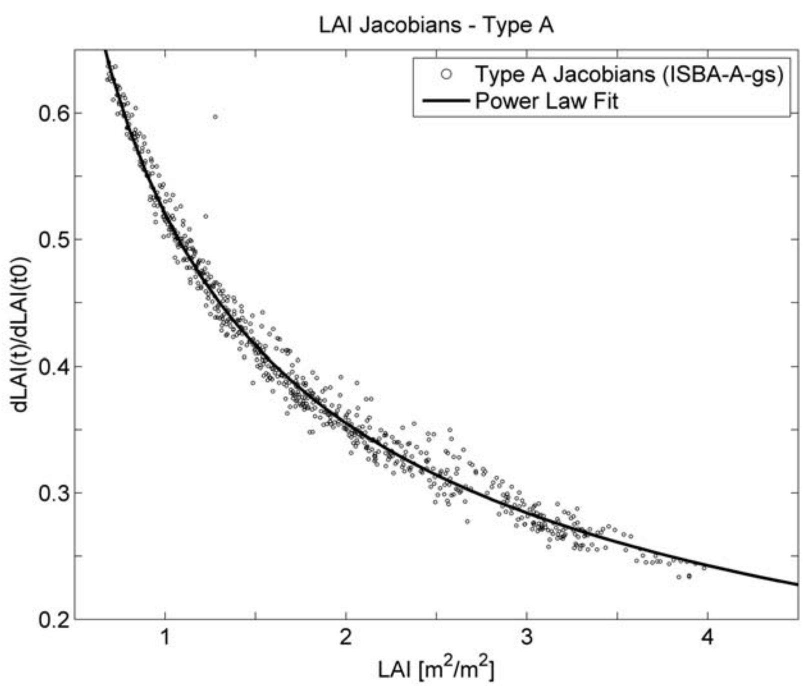

Figure 5. Dependence of type A LAI Jacobian values on LAI model states in 2001–2007. Type A corresponds to periods of vegetation growth and partial conversion of active biomass into structural biomass (see text for additional explanations). A power-law fit of a simple analytical formulation is also displayed [$d\mathrm{LAI}^{t}/d\mathrm{LAI}^{t_0} = 0.52(\mathrm{LAI}^{t_0})^{-0.55}$].

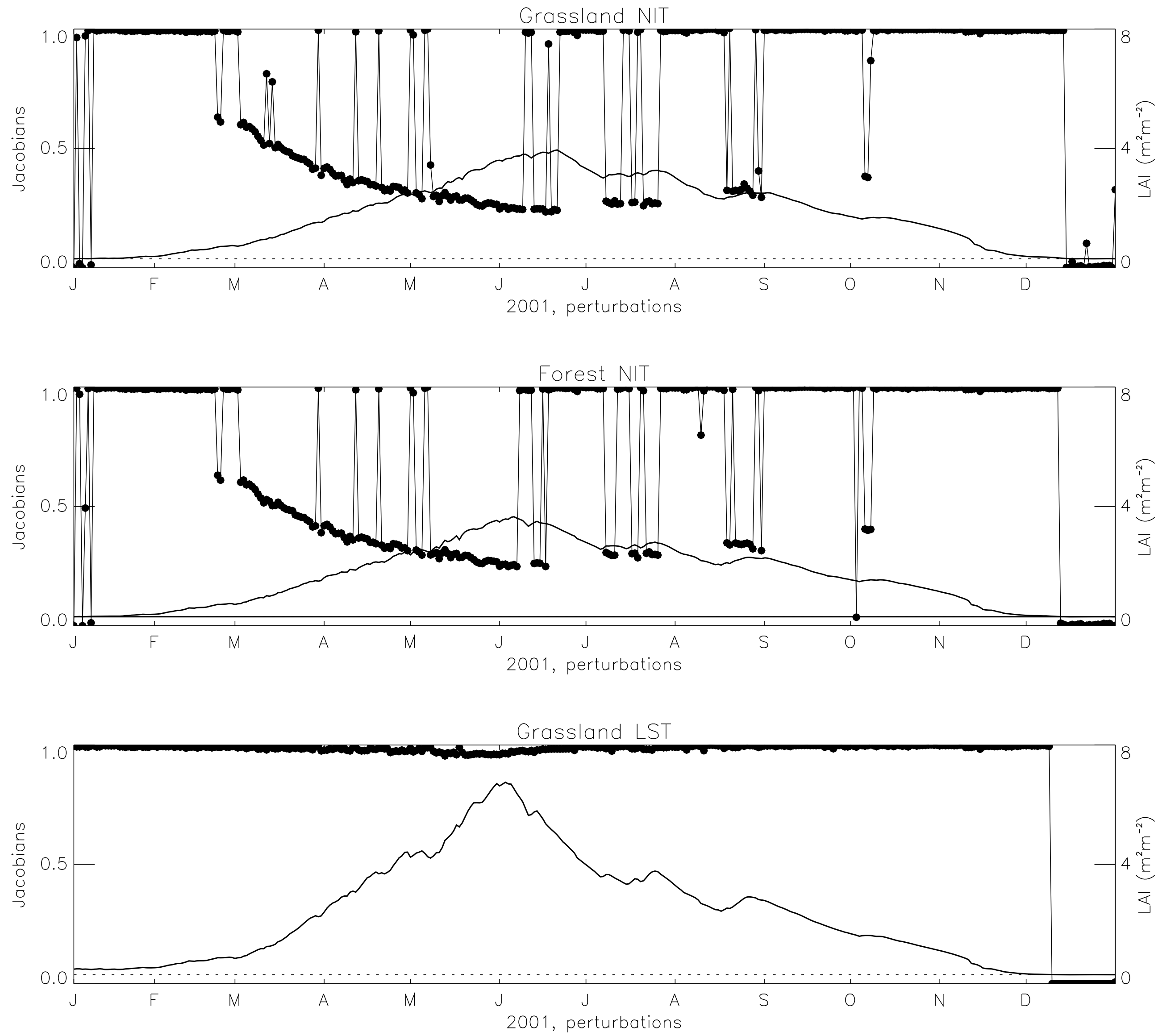

Figure 6. Time evolution of the LAI (thin line) and the Jacobian values (dots) in 2001 for ISBA-A-gs simulations using the SMOSREX forcing data with (a) grasslands (NIT version), (b) deciduous forests (NIT version), and (c) grasslands (LST version). The dashed line at LAI = 0.3 m^2/m^2 marks the model-imposed minimum LAI value.

[19] The aforementioned result suggests that the Jacobian may be expressed through a nonlinear function of the modeled LAI, that is, the model behavior itself. This is explained by studying the allometric logarithm equation contained in the nitrogen dilution module [*Calvet and Soussana*, 2001]. The Jacobian values of type A only occur during periods of vegetation growth, where the production of structural biomass exceeds the net loss of active biomass, which requires the inactive biomass to acquire biomass from the active biomass store. In ISBA-A-gs (NIT version), the total biomass is calculated through a mass balance of gains (photosynthesis) and losses (senescence and respiration of active biomass). The value of the total biomass allows the calculation of the active biomass by inverting the allometric logarithm equation, through which the previously prognostic model state of the active biomass B_a^t becomes a diagnostic variable. The formulation is thus

$$B_a^t = c\left(B_T^{t_0}\right)^{1-a}, \tag{6}$$

where B_T is the total biomass (sum of active and inactive biomass) and a is a curve parameter. As

$$B_T^{t_0} = B_a^{t_0} + B_s^{t_0}, \tag{7}$$

where B_s is the inactive or structural biomass, and assuming that B_s is independent of B_a, the Jacobian may be written as

$$\frac{d\mathrm{LAI}^t}{d\mathrm{LAI}^{t_0}} = \frac{dB_a^t}{dB_a^{t_0}} = c(1-a)\left(\frac{\mathrm{LAI}^{t_0}}{\alpha_B} + B_s^{t_0}\right)^{-a}. \tag{8}$$

Table 1. Vegetation Parameters Used in the Interaction Between the Soil, Biosphere and Atmosphere-A-gs Simulations for Grasslands and Deciduous Forests

Parameter	Symbol	Unit	Grasslands	Forests
Mesophyll conductance	g_m	mm/s	0.56	3
Critical extractable soil moisture	θ_c	%	50	30
Potential leaf life expectancy	τ	days	80	230
Minimum leaf area index	LAI_{min}	m^2/m^2	0.3	0.3
Cuticular conductance	g_c	mm/s	0.3	0.15
Nitrogen plasticity (slope)	e	m^2/(kg %)	5.84	4.83
Nitrogen plasticity (intercept)	f	m^2/kg	6.32	2.53
Leaf nitrogen concentration	N_l	%	1.4	2

The power law plotted in Figure 5 confirms this nonlinear dependence of the Jacobian with LAI. However, the fit gives a slightly larger negative exponent of −0.55 than the one given by the analytical Jacobian of equation (8) since a = 0.38 according to *Calvet and Soussana* [2001]. It means that additional dependences that have not been considered in the simple derivation above contribute to further decrease the active biomass within 1 day.

[20] These results have important implications for the data assimilation of remotely sensed LAI observations. The analysis increments ΔLAI are equal to the innovation vector times the Kalman gain k defined by

$$k = \frac{\sigma_b^2 h}{\sigma_o^2 + \sigma_b^2 h^2}, \tag{9}$$

where σ_b and σ_o are the standard deviations of background and observation errors, respectively.

[21] In the case of type B ($h \sim 1$) Jacobian values, the model dynamics (i.e., time dimension) does not bring any information to the analysis system: the analysis can be considered as static. Conversely, the type A Jacobian ($h < 1$) will lead to smaller analysis increments as soon as $\sigma_o < \sqrt{h\sigma_b}$ with the same observation and background errors as for type B.

4.5. Sensitivity of the Jacobian to Biome Specifications

[22] The results of the Jacobian sensitivity for two different biome specifications using the same nitrogen dilution model and climate conditions are presented on Figure 6 to examine the validity of the results previously presented for other vegetation types. Consequently, the grassland (herbaceous vegetation) present at SMOSREX was replaced with a deciduous forest (woody vegetation). In this case, the year 2001 is the most representative for temperate climates. The differences in the parameterization of the two vegetation types are summarized in Table 1.

[23] The results support the previous findings, with the woody vegetation showing a very similar response in the Jacobian values to those obtained for the herbaceous vegetation. In both cases, Jacobian values of the types A, B, and O are clearly identifiable. As for the grassland, the Jacobian values of the deciduous forest are 0 when the LAI is at its minimum threshold of 0.3 m^2/m^2 and of type A when the vegetation is in its growing phase. These results were expected, since the same nitrogen dilution model is used for both ecosystems.

4.6. Sensitivity of the Jacobian to Model Specifications

[24] To confirm the importance of the nitrogen dilution model for the behavior of the Jacobian values, a simulation run for the grasslands at SMOSREX has been performed with the LST version of ISBA-A-gs where this process is not described. As before, the year 2001 was chosen. A comparison of Figures 6a and 6c clearly shows that the main factor leading to a variation in Jacobian values is the nitrogen dilution model as discussed in section 4.4. Throughout the year, the Jacobian values in Figure 6c remain close to unity (i.e., type B response), while the winter response is identical to the full version of the model, as ISBA-A-gs requires to maintain the minimum LAI at 0.3 m^2/m^2 and any additional LAI is immediately removed from the active biomass component.

5. Conclusions

[25] This study has discussed the Jacobian values of the observation operator in an extended Kalman filter for assimilating LAI observations into the CO_2-responsive land surface model ISBA-A-gs in which the active biomass is the control variable (i.e., to be analyzed). Such examination is an important preliminary step for understanding the capacity of the assimilation system to ingest LAI observations. In comparison to previous studies, it was found that rather small perturbations (ε = 0.001) of the control variable (active biomass) led to accurate Jacobian values when using a finite-difference approximation and that large negative perturbations ($\varepsilon > 0.01$) resulted in considerable deviations from the expected behavior of the linearized model.

[26] The length of the assimilation interval was chosen to be 1 day in order to allow the joint assimilation of other observations available more frequently than LAI (e.g., soil moisture content, screen-level observations). Increasing the length to 10 days (availability of satellite LAI products and as used in previous studies) led to significantly reduced Jacobian values and consequently to a damping of the model's response at the end of the assimilation interval to the initial perturbations of the model states. Moreover, a length of 10 days for an assimilation interval would jeopardize near-real-time applications because of the very long cutoff needed to obtain the required observations. Such interval lengths also lead to a questioning of the linearity and perfect model assumptions when compared to shorter intervals. Since observations are only provided every 10 days without an exact knowledge of the observation times, the resulting uncertainty should be reflected in the observation error specification.

[27] The Jacobian appears to have two types of contrasted values, one in which all or none of the perturbed active biomass is kept by the model, and a second in which a fraction of the active biomass is converted into structural biomass. It was shown that values associated with types O and B (the Jacobian being 0 or 1, respectively) occur during specific periods of the vegetation activity, notably during periods when vegetation activity is strongly reduced, due to water stress, strong plant senescence, or cold, cloudy, and rainy conditions. Conversely, Jacobian values of type A (the Jacobian being between 0 and 1) occur during phases of net carbon assimilation into the plant, that is, during periods of vegetation growth. As those findings mean that parts of the

added active biomass are converted into structural biomass for type A conditions (nitrogen dilution module), it is suggested that this effect on the overall model behavior should be carefully examined in the context of the assimilation of LAI observations into a land surface model. These conclusions are relevant not only for ISBA-A-gs, but also for other land surface models that utilize the same nitrogen dilution scheme, for example, C-TESSEL of ECMWF [*Lafont et al.*, 2007; *Jarlan et al.*, 2008].

[28] These results have important implications for the assimilation of LAI observations into a LSM. The analysis increments depend not only on perturbation sizes and defined errors, but also on the plant physiological activity. As perturbation sizes have been defined as proportional to the amount of active biomass, the background error definition may require a similar adaptation. *Sabater et al.* [2008] defined the observation and background errors as a constant 1 m^2/m^2, while *Jarlan et al.* [2008] introduced a variable model error of 20% of the forecast LAI state. The results of this study support the findings of *Jarlan et al.* [2008], as they underline the need for a variable error definition. Consequently, it is recommended to improve both error definitions; for example, to define them not only as a function of the amount of photosynthetically active biomass, but also of the plant's activity, expressed through the net assimilation of CO_2.

[29] **Acknowledgments.** C.R. was supported by an Australian Research Council Discovery Project grant (DP0879212). C.A.'s doctoral fellowship is cofinanced by CNES. J.W.'s visit to CNRM was supported by the STAE (Sciences et Technologies pour l'Aéronautique et l'Espace) foundation in the framework of the CYMENT project. This work is a contribution to the geoland2 project, cofunded by the European Commission within the GMES initiative in FP7. The authors wish to thank Lionel Jarlan, Karim Bergaoui, and Clara Draper for their contributions in coding the initial 2D-VAR/EKF versions.

References

Balsamo, G., F. Bouyssel, and J. Noilhan (2004), A simplified bi-dimensional variational analysis of soil moisture from screen-level observations in a mesoscale numerical weather prediction model, *Q. J. R. Meteorol. Soc.*, *130*, 895–915, doi:10.1256/qj.02.215.

Berg, A., J. Famiglietti, J. Walker, and P. R. Houser (2003), Impact of bias correction to reanalysis products on simulations of North American soil moisture and hydrological fluxes, *J. Geophys. Res.*, *108*(D16), 4490, doi:10.1029/2002JD003334.

Bubnová, R., G. Hello, P. Bénard, and J. F. Geleyn (1995), Integration of the fully elastic equations cast in the hydrostatic pressure terrain-following coordinate in the framework of the ARPEGE/Aladin NWP system, *Mon. Weather Rev.*, *123*, 515–535, doi:10.1175/1520-0493(1995)123<0515:IOTFEE>2.0.CO;2.

Calvet, J.-C. (2000), Investigating soil and atmospheric plant water stress using physiological and micrometeorological data, *Agric. Forest Meteorol.*, *103*, 229–247, doi:10.1016/S0168-1923(00)00130-1.

Calvet, J.-C., and J.-F. Soussana (2001), Modelling CO_2-enrichment effects using an interactive vegetation SVAT scheme, *Agric. Forest Meteorol.*, *108*, 129–152, doi:10.1016/S0168-1923(01)00235-0.

Calvet, J.-C., J. Noilhan, J.-L. Roujean, P. Bessemoulin, M. Cabelguenne, A. Olioso, and J.-P. Wigneron (1998), An interactive vegetation model tested against data from six contrasting sites, *Agric. Forest Meteorol.*, *92*, 73–95, doi:10.1016/S0168-1923(98)00091-4.

Calvet, J.-C., V. Rivalland, C. Picon-Cochard, and J.-M. Guehl (2004), Modelling forest transpiration and CO_2 fluxes: Response to soil water stress, *Agric. Forest Meteorol.*, *124*, 143–156, doi:10.1016/j.agrformet.2004.01.007.

Chevallier, F., and J.-F. Mahfouf (2001), Evaluation of Jacobians of infrared models for variational assimilation, *J. Appl. Meteorol.*, *40*, 1445–1462, doi:10.1175/1520-0450(2001)040<1445:EOTJOI>2.0.CO;2.

Crow, W. T., R. D. Koster, R. H. Reichle, and H. O. Sharif (2005), Relevance of time-varying and time-invariant retrieval error sources on the utility of spaceborne soil moisture products, *Geophys. Res. Lett.*, *32*, L24405, doi:10.1029/2005GL024889.

De Lannoy, G. J. M., R. H. Reichle, P. R. Houser, V. R. N. Pauwels, and N. E. C. Verhoest (2007), Correcting for forecast bias in soil moisture assimilation with the ensemble Kalman filter, *Water Resour. Res.*, *43*, W09410, doi:10.1029/2006WR005449.

Dente, L., G. Satalino, F. Mattia, and M. Rinaldi (2008), Assimilation of leaf area index derived from ASAR and MERIS data into CERES-Wheat model to map wheat yield, *Remote Sens. Environ.*, *112*, 1395–1407, doi:10.1016/j.rse.2007.05.023.

De Rosnay, P., et al. (2006), SMOSREX: A long term field campaign experiment for soil moisture and land surface processes, *Remote Sens. Environ.*, *102*, 377–389, doi:10.1016/j.rse.2006.02.021.

Draper, C. S., J.-F. Mahfouf, and J. P. Walker (2009), An EKF assimilation of AMSR-E soil moisture into the ISBA land surface scheme, *J. Geophys. Res.*, *114*, D20104, doi:10.1029/2008JD011650.

Drusch, M., E. F. Wood, and H. Gao (2005), Observation operators for the direct assimilation of TRMM microwave imager retrieved soil moisture, *Geophys. Res. Lett.*, *32*, L15403, doi:10.1029/2005GL023623.

Fillion, L., and J.-F. Mahfouf (2003), Jacobians of an operational prognostic cloud scheme, *Mon. Weather Rev.*, *131*, 2838–2856, doi:10.1175/1520-0493(2003)131<2838:JOAOPC>2.0.CO;2.

Garand, L., et al. (2001), Radiance and Jacobian intercomparison of radiative transfer models applied to HIRS and AMSU channels, *J. Geophys. Res.*, *106*, 24,017–24,031, doi:10.1029/2000JD000184.

Giard, D., and E. Bazile (2000), Implementation of a new assimilation scheme for soil and surface variables in a global NWP model, *Mon. Weather Rev.*, *128*, 997–1015, doi:10.1175/1520-0493(2000)128<0997:IOANAS>2.0.CO;2.

Jacobs, C. M. J., B. J. J. M. van den Hurk, and H. A. R. de Bruin (1996), Stomatal behaviour and photosynthetic rate of unstressed grapevines in semi-arid conditions, *Agric. Forest Meteorol.*, *80*, 111–134, doi:10.1016/0168-1923(95)02295-3.

Jarlan, L., G. Balsamo, S. Lafont, A. Beljaars, J.-C. Calvet, and E. Mougin (2008), Analysis of leaf area index in the ECMWF land surface model and impact on latent heat and carbon fluxes: Application to West Africa, *J. Geophys. Res.*, *113*, D24117, doi:10.1029/2007JD009370.

Krinner, G., N. Viovy, N. De Noblet-Ducoudré, J. Ogée, J. Polcher, P. Friedlingstein, P. Ciais, S. Sitch, and I. C. Prentice (2005), A dynamic global vegetation model for studies of the coupled atmosphere-biosphere system, *Global Biogeochem. Cycles*, *19*, GB1015, doi:10.1029/2003GB002199.

Lafont, S., M. Voogt, A. Beljaars, B. J. J. M. van den Hurk, L. Jarlan, and G. Balsamo (2007), Description and evaluation of the carbon version of TESSEL: CTESSEL model, *ECMWF Tech. Memo.*, 37 pp., Eur. Cent. for Medium-Range Weather Forecasts, Reading, U. K.

Lemaire, G., and F. Gastal (1997), N uptake and distribution in plant canopies, in *Diagnosis of the Nitrogen Status in Crops*, edited by G. Lemaire, pp. 3–43, Springer, Berlin.

Le Moigne, P. (2009), SURFEX scientific documentation, *Note de Cent. du Groupe de Météorol. à Moyenne Echelle 87*, 211 pp., CNRM/Météo-France, Toulouse, France.

Mahfouf, J.-F., K. Bergaoui, C. Draper, F. Bouyssel, F. Taillefer, and L. Taseva (2009), A comparison of two off-line soil analysis schemes for assimilation of screen level observations, *J. Geophys. Res.*, *114*, D08105, doi:10.1029/2008JD011077.

Noilhan, J., and J.-F. Mahfouf (1996), The ISBA land surface parameterization scheme, *Global Planet. Change*, *13*, 145–159, doi:10.1016/0921-8181(95)00043-7.

Noilhan, J., and S. Planton (1989), A simple parameterization of land surface processes for meteorological models, *Mon. Weather Rev.*, *117*, 536–549, doi:10.1175/1520-0493(1989)117<0536:ASPOLS>2.0.CO;2.

Reichle, R. H., and R. Koster (2004), Bias reduction in short records of satellite soil moisture, *Geophys. Res. Lett.*, *32*, L19501, doi:10.1029/2004GL020938.

Reichle, R. H., D. B. McLaughlin, and D. Entekhabi (2002), Hydrologic data assimilation with the ensemble Kalman filter, *Mon. Weather Rev.*, *130*, 103–114, doi:10.1175/1520-0493(2002)130<0103:HDAWTE>2.0.CO;2.

Sabater, J. M., L. Jarlan, J.-C. Calvet, F. Bouyssel, and P. De Rosnay (2007), From near surface to root zone soil moisture using different assimilation techniques, *J. Hydrometeorol.*, *8*, 194–206, doi:10.1175/JHM571.1.

Sabater, J. M., C. Rüdiger, J.-C. Calvet, N. Fritz, L. Jarlan, and Y.-H. Kerr (2008), Joint assimilation of surface moisture and LAI observations into a land surface model, *Agric. Forest Meteorol.*, *148*, 1362–1373, doi:10.1016/j.agrformet.2008.04.003.

Walker, J. P., and P. R. Houser (2001), A methodology for intializing soil moisture in a global climate model: Assimilation of near-surface soil moisture observations, *J. Geophys. Res.*, *106*, 11,761–11,774, doi:10.1029/2001JD900149.

Walker, J. P., G. R. Willgoose, and J. D. Kalma (2001), One-dimensional soil moisture profile retrieval by assimilation of near-surface measurements: A simplified soil moisture model and field application, *J. Hydrometeorol.*, *2*, 356–373, doi:10.1175/1525-7541(2001)002<0356:ODSMPR>2.0.CO;2.

C. Albergel, J.-C. Calvet, and J.-F. Mahfouf, Centre National de Recherches Météorologiques, Météo-France/CNRS, Toulouse 31057, France.

C. Rüdiger and J. P. Walker, Department of Civil Engineering, Monash University, Clayton, Victoria 3800, Australia. (crudiger@unimelb.edu.au)